In-plane surface phonon-polariton thermal conduction in dielectric multilayer systems

S Tachikawa, J Ordonez-Miranda, Y Wu, L Jalabert, R Anufriev, Sebastian Volz, M Nomura

Applied Physics Letters

In-plane surface phonon-polariton thermal conduction in dielectric multilayer systems

Cite as: Appl. Phys. Lett. **121**, 202202 (2022); https://doi.org/10.1063/5.0117081
Submitted: 30 July 2022 • Accepted: 23 October 2022 • Published Online: 14 November 2022

S. Tachikawa, J. Ordonez-Miranda, Y. Wu, et al.

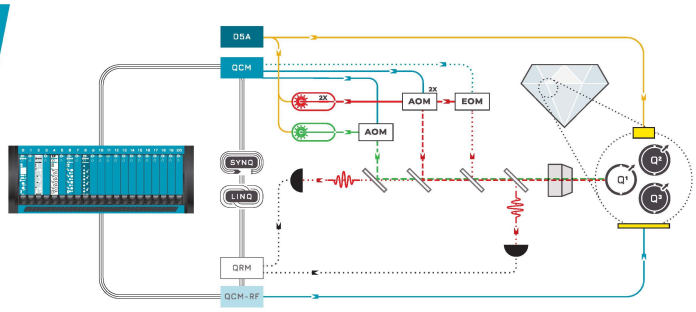

AIP Publishing

Applied Physics Letters ARTICLE scitation.org/journal/apl

In-plane surface phonon-polariton thermal conduction in dielectric multilayer systems

Cite as: Appl. Phys. Lett. **121**, 202202 (2022); doi: 10.1063/5.0117081
Submitted: 30 July 2022 · Accepted: 23 October 2022 ·
Published Online: 14 November 2022

S. Tachikawa,[1,a)] J. Ordonez-Miranda,[1,2] Y. Wu,[1] L. Jalabert,[1,2] R. Anufriev,[1] S. Volz,[1,2,a)] and M. Nomura[1,2,a)]

AFFILIATIONS

[1]Institute of Industrial Science, The University of Tokyo, Tokyo 153-8505, Japan
[2]LIMMS, CNRS-IIS IRL 2820, The University of Tokyo, Tokyo 153-8505, Japan

Note: This paper is part of the APL Special Collection on Thermal Radiation at the Nanoscale and Applications.
[a)]**Authors to whom correspondence should be addressed:** saekotac@iis.u-tokyo.ac.jp; volz@iis.u-tokyo.ac.jp; and nomura@iis.u-tokyo.ac.jp

ABSTRACT

Nanoscale heat conduction is limited by surface scattering of phonons but can be enhanced by surface phonon-polaritons (SPhPs), which are the hybridization of photons and optical phonons in polar materials. Here, we analyze the dispersion of SPhPs in a multilayer system consisting of a silicon (Si) layer sandwiched between two silicon dioxide (SiO_2) nanolayers. We find that SPhPs generated in SiO_2 nanolayers couple with guided resonant modes and propagate mainly in the nonabsorbent Si layer for microscale Si thicknesses. This coupling yields an enhancement in thermal conductivity with Si thickness. In contrast, for nanoscale Si thicknesses, evanescent components of SPhPs couple inside the Si layer, resulting in a higher thermal conductivity for thinner Si layers. The transition between these two different coupling phenomena provides the minimum of the in-plane SPhP thermal conductivity at a Si thickness of approximately 1 μm. Our finding brings deeper insight into thermal management in electronics and semiconductors.

Modern semiconductor technology enables fabrication of nanoscale devices. The high density of elements in electrical circuits causes local heating on semiconductor chips, which damages devices and lowers their performance.[1] Nanoscale structures suppress the phonon transport, resulting in restrained heat dissipation.[2–6] Local heating has, thus, become a critical issue, and alternative cooling solutions relevant to the nanoscale are in great need.

Meanwhile, surface phonon-polaritons (SPhPs) are of interest as another effective heat carriers at the nanoscale.[2,7–9] Surface phonon-polaritons are surface waves of polar materials, generated by photons and optical phonons hybridizing in the infrared range. In nanofilms, due to the high surface-to-volume ratio, SPhP propagation lengths can reach up to a few hundred micrometers.[2,10] Thus, SPhPs can dominate the in-plane thermal transport.[2,9–12] Experimental works have revealed the high thermal property of SPhPs in silicon dioxide and silicon nitride nanofilms.[13,14] However, suspending a nanometric film is technically challenging, and such a geometry is impractical for applications. Researchers have studied SPhP propagation and in-plane thermal transfer in multilayer systems,[16,17] yet the physical description of SPhP thermal transport remains incomplete. It is also to note that nanometric layers were considered to achieve high thermal property by lowering absorption.[2,10,16,17]

In this work, we consider a multilayer system in which relatively thick silicon (Si) is sandwiched between silicon dioxide (SiO_2) nanolayers [Fig. 1(a)]. We expect the SPhPs, excited in both top and bottom SiO_2 layers, to couple inside the Si layer, which is an SPhP non-active material. Thus, the configuration promotes heat conduction.[18] With this aim, we investigate the Si thickness dependence on SPhP in-plane thermal transport in a multilayer system of SPhP active and non-active materials. Figure 1(a) provides the schematic of our SiO_2/Si/SiO_2 three-layer system. The permittivities of silicon, silicon dioxide, and vacuum are expressed as ε_{Si}, ε_{SiO_2}, and ε_0, respectively. We define the in-plane wave vector of the electromagnetic field along the interface as β and the cross-plane wave vector as

$$p^2_{Si,SiO_2} = \beta^2 - \varepsilon_{Si,SiO_2} k_0^2, \tag{1}$$

where $k_0 = \frac{\omega}{c}$, with ω being the spectral frequency of SPhP propagation and c being the speed of light in vacuum. Silicon thickness dependence of the in-plane wave vector can be seen in supplementary

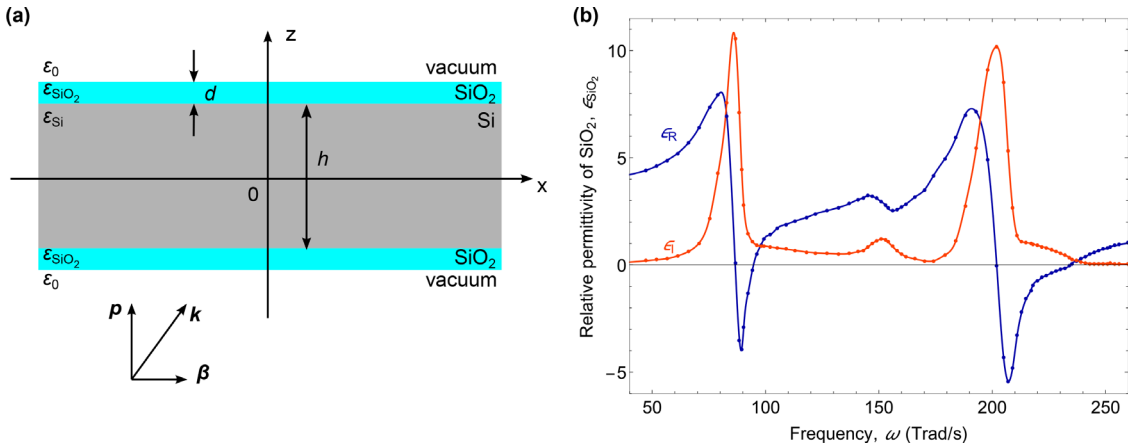

FIG. 1. (a) Cross-plane schematic of the SiO_2/Si/SiO_2 three-layer system. The permittivity for vacuum, Si, and SiO_2 are defined as ε_0, ε_{Si}, and ε_{SiO_2}, respectively. (b) Experimental values of the real and imaginary parts of the SiO_2 relative permittivity reported in the literature.[15]

material 3. By solving the Maxwell equation with the proper boundary conditions of tangential component continuity, the dispersion relation of SPhPs in the three-layer system is described along two solutions as detailed below (see supplementary material 1).

The symmetric one reads as

$$\left[\frac{p_0\varepsilon_{SiO_2}}{p_{SiO_2}\varepsilon_0}\tanh(p_{SiO_2}d)+1\right]\tanh(p_{Si}h/2) + \frac{p_{SiO_2}\varepsilon_{Si}}{p_{Si}\varepsilon_{SiO_2}}\left[\frac{p_0\varepsilon_{SiO_2}}{p_{SiO_2}\varepsilon_0}+\tanh(p_{SiO_2}d)\right]=0. \quad (2)$$

The asymmetric one is as

$$\left[\frac{p_0\varepsilon_{SiO_2}}{p_{SiO_2}\varepsilon_0}+\tanh(p_{SiO_2}d)\right]\tanh(p_{Si}h/2) + \frac{p_{Si}\varepsilon_{SiO_2}}{p_{SiO_2}\varepsilon_{Si}}\left[\frac{p_0\varepsilon_{SiO_2}}{p_{SiO_2}\varepsilon_0}\tanh(p_{SiO_2}d)+1\right]=0, \quad (3)$$

where d and h are SiO_2 and Si thicknesses, respectively.

The relative permittivity of SiO_2 is shown in Fig. 1(b). The peaks at 87 and 202 Trad/s indicate that SiO_2 absorbs a significant amount of energy from the electromagnetic field and can couple to form polaritons in the range of those resonant frequencies. In our calculations, we use the complex permittivity of SiO_2 shown in Fig. 1(b) for the SPhP active material and the constant relative permittivities of $\varepsilon_{Si} = 11.7$ and $\varepsilon_0 = 1$ for the SPhP non-active materials.

We calculate the dispersion relation of SPhPs in the three-layer system using the Si and SiO_2 thicknesses of $d = 30$ nm and $h = 10\,\mu$m. Figure 2(a) shows the derived dispersion relation of the real part of β, β_R. Multiple branches were obtained from symmetric and asymmetric solutions. This is due to the term $\tanh(p_{Si}h/2)$. In previous studies on nanometric films where the condition $|p_{SiO_2}|d \ll 1$ was satisfied, the simplification of $\tanh(x) \to x$ provided only one solution. However, with a relatively high value of $h = 10\,\mu$m, the hyperbolic tangent, $\tanh(p_{Si}h/2)$, cannot be reduced to a linear term and, thus, provides multiple branches, which correspond to the partially confined modes in the cross-plane direction. All the branches are below the light line in vacuum (black dashed line), which indicates that they are evanescent in air throughout the frequency range. They are also slower than SPhP in a single SiO_2 film of 30 nm thickness (black solid line), which is superposed with the vacuum light line.

To study further the SPhP in the three-layer system, we analyzed the dispersion relation for different Si thicknesses h. Figure 2(b) shows the comparison of the first branch of the symmetric solution derived for various values of h. For thicker Si, the dispersion curve follows the light line in Si (gray dashed line), whereas for thinner Si, it follows the light line in vacuum (black dashed line), typically below $h = 1\,\mu$m. This behavior comes from the fact that for thicker Si, the SPhPs couple with the guided resonant modes of Si, whereas for thinner Si, the SPhPs behave like those along a single SiO_2 film. In the latter case, the SPhP energy is mainly distributed in vacuum space, as shown in Fig. 3. These two regimes will be further discussed in the following paragraphs.

Next, we derive the in-plane SPhP thermal conductivity of the three-layer system. In-plane propagation length Λ is defined using the imaginary part of the in-plane wave vector, β_I as[2]

$$\Lambda = \frac{1}{2\beta_I}. \quad (4)$$

In-plane propagation in the three-layer system as a function of the Si thickness h is plotted in Fig. 2(c) for the first branch of the symmetric and asymmetric solutions. Both solutions reveal a decrease with the Si thickness. The SPhP in-plane propagation length spectrum of each branch of the three-layer system is also studied (see supplementary material 2). However, as Si becomes thinner than 1.1 μm (2.3 μm for the asymmetric solution), Λ increases as h decreases. The results also indicate a minimum of Λ. Note that for $h < 1.1\,\mu$m, $\tanh(p_{Si}h/2)$ can be reduced to $p_{Si}h/2$, and there is only one branch from the symmetric solution. In-plane thermal conductivity κ of SPhPs is described by summation of different modes j, using β_R and Λ as

$$\kappa = \frac{1}{4\pi(h+2d)}\sum_j \int_0^\infty \hbar\omega\Lambda_j\beta_{R,j}\frac{\partial f_0}{\partial T}d\omega, \quad (5)$$

where f_0 is the Bose–Einstein distribution function.[2]

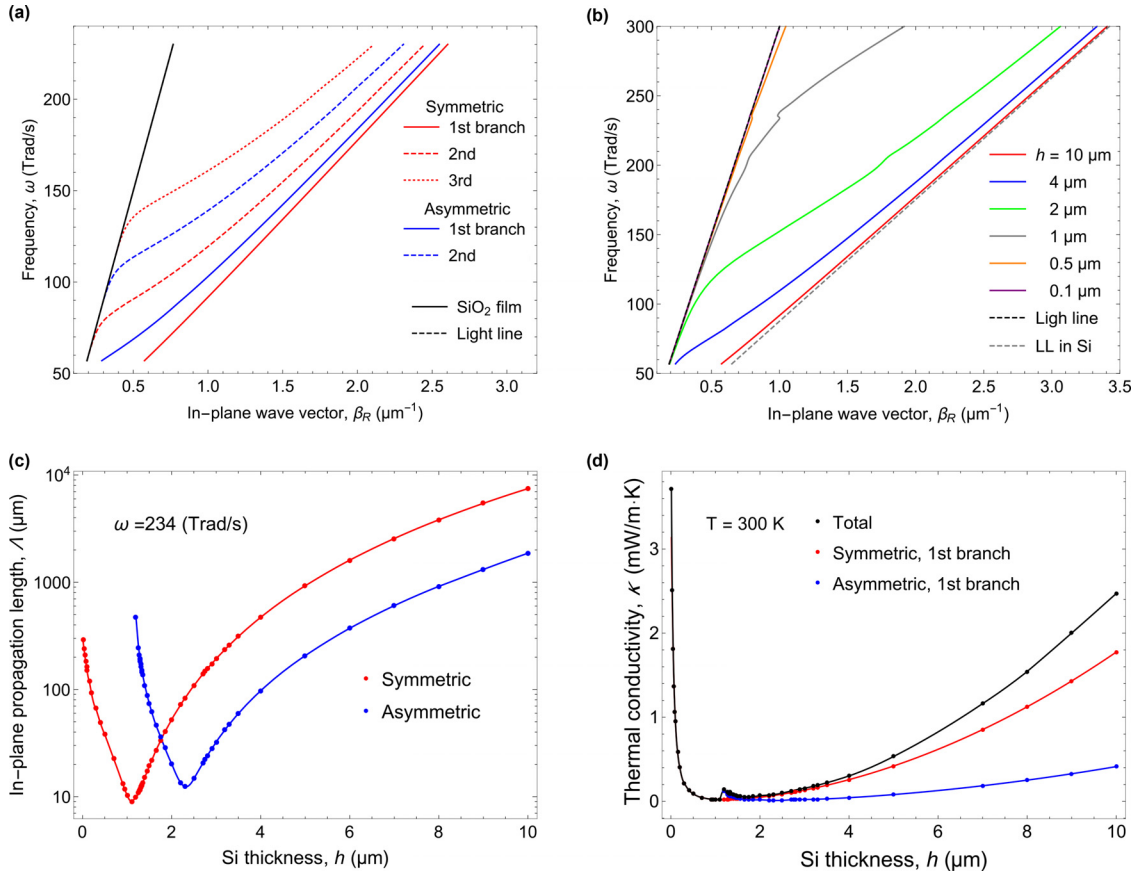

FIG. 2. (a) The dispersion relation of SPhPs in the three-layer system with SiO_2 and Si thicknesses of $d = 30$ nm and $h = 10\ \mu$m. Both symmetric and asymmetric solutions provide multiple branches, and they are all below the light line in a vacuum, plotted in the black dashed line. All branches were slower than the case of SPhP in the SiO_2 single film of 30 nm thickness (plotted in the solid black line), which almost superposes with the light line in a vacuum. (b) The first branch of the symmetric solution of β_R for the different values of Si thicknesses h. In thicker Si, dispersion curves are brought along the Si light line (gray dashed line), whereas they come along the light line in a vacuum (black dashed line) when the Si thickness reduces. (c) Si thickness dependence of the SPhP in-plane propagation length. The first branch of the symmetric and asymmetric solutions is compared at a frequency of $\omega = 234$ Trad/s. (d) Si thickness dependence of the in-plane SPhP thermal conductivity. The contribution from the multiple branches is summed up to derive the total thermal conductivity.

The Si thickness dependence of the in-plane SPhP thermal conductivity is plotted in Fig. 2(d). As thick Si films yield multiple solutions, the thermal conductivity is calculated by summing up the contributions from multiple branches. Contribution of the high-order branches to the thermal conductivity can be seen in supplementary material 4. Following the trend of Λ shown in Fig. 2(c), the in-plane thermal conductivity also displays a minimum of around 1 μm.

Two regimes clearly appear, i.e., when $h > 1\ \mu$m and $h < 1\ \mu$m. To discuss the physical background causing two different regimes, we analyzed the SPhP energy distribution in the three-layer system. Figure 3 shows the SPhP in-plane Poynting vector for $h = 0.1$, 0.5, 1, and 10 μm. The SPhP Poynting vector in the x direction (S_x) was calculated by taking the real part of the electric field in the z direction (E_z) multiplied with the conjugate of the magnetic field in the y direction (H_y^*) as

$$S_x = \frac{1}{2}\Re\left[E_z \times H_y^*\right]. \tag{6}$$

For $h = 10\ \mu$m, the SPhP energy is mainly distributed inside the Si layer. Surface phonon polaritons excited in the SiO_2 layers couple with propagative waves inside the nonabsorbent Si layer and couple with the guided resonant modes. Thus, multiple solutions are obtained for a thicker Si layer.

When $h = 1\ \mu$m, the SPhPs are still coupled with the Si-guided resonant modes and distribute its energy in the Si layer, but with less value and the number of branches is reduced compared to the thicker Si case. For $h < 1\ \mu$m, propagative waves can no longer exist inside the thin Si layer, and SPhPs excited in the SiO_2 layers can be proven to evanescently couple inside the Si layer. Most of the energy is distributed along the vacuum/SiO_2 interface, and the profile is similar to the one of the single film case. This profile corresponds to the fact that the dispersion curve of β_R for $h < 1\ \mu$m was along the light line in a vacuum, as is also the case for the SiO_2 single film [Fig. 2(b)]. As the Si thickness decreases, the energy distribution is more widely spread in the nonabsorbent vacuum, therefore yielding a longer propagation length and a higher thermal conductivity for thinner Si films.

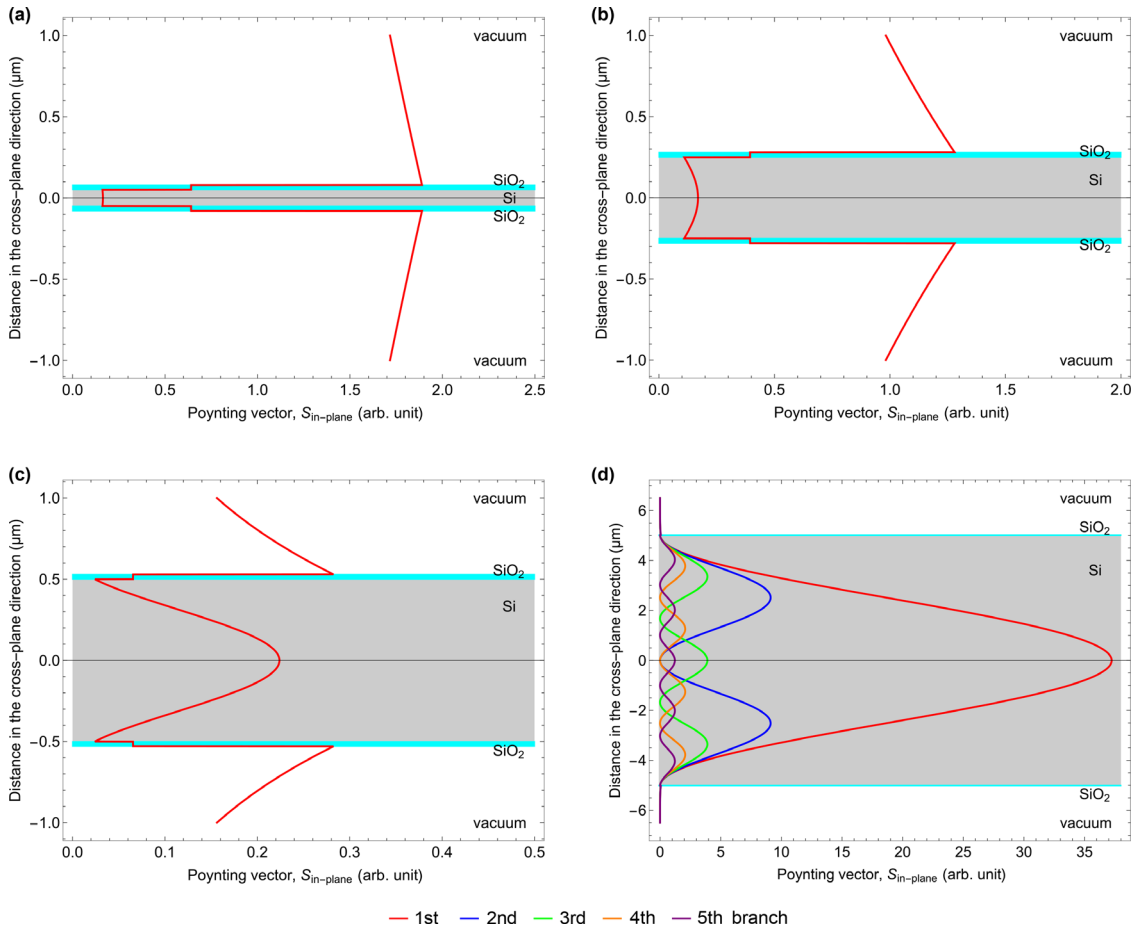

FIG. 3. The SPhP energy profile for the Si thickness of (a) $h = 0.1$, (b) 0.5, (c) 1, and (d) 10 μm.

In this work, we analyzed the propagation and thermal transfer of SPhPs in a SiO_2/Si/SiO_2 multilayer system. We found that, in the range of microscale Si thicknesses, SPhPs generated inside the SiO_2 nanolayers couple with the guided resonant modes of the Si layer, and the SPhP energy propagates inside the nonabsorbent Si layer mainly. This coupling leads to the SPhP propagation length and the thermal conductivity reduction by thinning the Si layer. On the other hand, when Si becomes thinner than 1 μm, propagative waves can no longer exist across the Si layer, and SPhPs generated in the top and bottom SiO_2 couple inside the Si layer via evanescent waves. In this second coupling regime, the multilayer system tends to behave like a single film, resulting in a higher thermal conductivity for thinner Si layers. The transition between these two coupling regimes yields a minimum for the SPhP in-plane propagation length and thermal conductivity. We have finally revealed the complex set of mechanisms in the in-plane heat flux due to the coupling between surface phonon-polaritons and resonant guided modes. This finding brings in a deeper understanding of thermal conduction in solids that will impact the thermal management of micro- and nanosystems.

See the supplementary material for the detailed information about the theoretical background.

This work was supported by CREST JST (Grant Nos. JPMJCR19I1 and JPMJCR19Q3), KAKENHI JSPS (Grant Nos. 21H04635 and JP20J13729), and the JSPS Core-to-Core Program (Grant No. JPJSCCA20190006).

AUTHOR DECLARATIONS

Conflict of Interest

The authors have no conflicts to disclose.

Author Contributions

Saeko Tachikawa: Formal analysis (equal); Investigation (equal); Writing – original draft (equal). **Jose Ordonez-Miranda:** Data curation (equal); Validation (equal); Writing – review & editing (equal). **Yunhui Wu:** Investigation (supporting); Writing – review & editing (equal). **Laurent Jalabert:** Writing – review & editing (supporting). **Roman Anufriev:** Writing – review & editing (equal). **Sebastian Volz:**

Funding acquisition (equal); Supervision (equal); Writing – review & editing (equal). **Masahiro Nomura:** Funding acquisition (equal); Supervision (equal); Writing – review & editing (equal).

DATA AVAILABILITY

The data that support the findings of this study are available from the corresponding authors upon reasonable request.

REFERENCES

[1]O. Semenov, A. Vassighi, and M. Sachdev, "Impact of self-heating effect on long-term reliability and performance degradation in CMOS circuits," IEEE Trans. Device Mater. Rel. **6**, 17–27 (2006).

[2]D.-Z. A. Chen, A. Narayanaswamy, and G. Chen, "Surface phonon-polariton mediated thermal conductivity enhancement of amorphous thin films," Phys. Rev. B **72**, 155435 (2005).

[3]J. L. Braun, C. H. Baker, A. Giri, M. Elahi, K. Artyushkova, T. E. Beechem, P. M. Norris, Z. C. Leseman, J. T. Gaskins, and P. E. Hopkins, "Size effects on the thermal conductivity of amorphous silicon thin films," Phys. Rev. B **93**, 140201 (2016).

[4]S. Volz, J. Ordonez-Miranda, A. Shchepetov, M. Prunnila, J. Ahopelto, T. Pezeril, G. Vaudel, V. Gusev, P. Ruello, E. M. Weig *et al.*, "Nanophononics: State of the art and perspectives," Eur. Phys. J. B **89**, 15 (2016).

[5]M. Nomura, J. Shiomi, T. Shiga, and R. Anufriev, "Thermal phonon engineering by tailored nanostructures," Jpn. J. Appl. Phys., Part 1 **57**, 080101 (2018).

[6]M. Nomura, R. Anufriev, Z. Zhang, J. Maire, Y. Guo, R. Yanagisawa, and S. Volz, "Review of thermal transport in phononic crystals," Mater. Today Phys. **22**, 100613 (2022).

[7]F. Yang, J. Sambles, and G. Bradberry, "Long-range surface modes supported by thin films," Phys. Rev. B **44**, 5855 (1991).

[8]J.-J. Greffet, R. Carminati, K. Joulain, J.-P. Mulet, S. Mainguy, and Y. Chen, "Coherent emission of light by thermal sources," Nature **416**, 61–64 (2002).

[9]D.-Z. A. Chen and G. Chen, "Measurement of silicon dioxide surface phonon-polariton propagation length by attenuated total reflection," Appl. Phys. Lett. **91**, 121906 (2007).

[10]J. Ordonez-Miranda, L. Tranchant, T. Tokunaga, B. Kim, B. Palpant, Y. Chalopin, T. Antoni, and S. Volz, "Anomalous thermal conductivity by surface phonon-polaritons of polar nano thin films due to their asymmetric surrounding media," J. Appl. Phys. **113**, 084311 (2013).

[11]D.-Z. A. Chen and G. Chen, "Heat flow in thin films via surface phonon-polaritons," Front. Heat Mass Transfer **1**, 023005 (2010).

[12]S. Gluchko, B. Palpant, S. Volz, R. Braive, and T. Antoni, "Thermal excitation of broadband and long-range surface waves on SiO_2 submicron films," Appl. Phys. Lett. **110**, 263108 (2017).

[13]L. Tranchant, S. Hamamura, J. Ordonez-Miranda, T. Yabuki, A. Vega-Flick, F. Cervantes-Alvarez, J. J. Alvarado-Gil, S. Volz, and K. Miyazaki, "Two-dimensional phonon polariton heat transport," Nano Lett. **19**, 6924–6930 (2019).

[14]Y. Wu, J. Ordonez-Miranda, S. Gluchko, R. Anufriev, D. D. S. Meneses, L. Del Campo, S. Volz, and M. Nomura, "Enhanced thermal conduction by surface phonon-polaritons," Sci. Adv. **6**, eabb4461 (2020).

[15]E. D. Palik, *Handbook of Optical Constants of Solids* (Academic Press, 1998), Vol. 3.

[16]J. Ordonez-Miranda, L. Tranchant, Y. Chalopin, T. Antoni, and S. Volz, "Thermal conductivity of nano-layered systems due to surface phonon-polaritons," J. Appl. Phys. **115**, 054311 (2014).

[17]M. Lim, J. Ordonez-Miranda, S. S. Lee, B. J. Lee, and S. Volz, "Thermal-conductivity enhancement by surface electromagnetic waves propagating along multilayered structures with asymmetric surrounding media," Phys. Rev. Appl. **12**, 034044 (2019).

[18]S. Tachikawa, J. Ordonez-Miranda, Y. Wu, L. Jalabert, R. Anufriev, S. Volz, and M. Nomura, "High surface phonon-polariton in-plane thermal conductance along coupled films," Nanomaterials **10**, 1383 (2020).